International Journal of Heat and Mass Transfer xxx (xxxx) xxx

Contents lists available at ScienceDirect

International Journal of Heat and Mass Transfer

journal homepage: www.elsevier.com/locate/ijhmt

Model and sensitivity analysis of the reciprocating biomass conversion reactor (RBCR)

N.J. Parziale, R. Adhikari

Castle Point on Hudson, Stevens Institute of Technology, Hoboken, NJ 07030, USA

ARTICLE INFO

Article history:
Received 13 June 2019
Received in revised form 1 November 2019
Accepted 2 November 2019
Available online xxxx

2010 MSC classification:
00-01
99-00

ABSTRACT

In this work, the capabilities of a pilot-scale reciprocating biomass conversion reactor (RBCR) are assessed by modeling. The RBCR is a novel means to produce bio-oil by fast-pyrolysis whose core is a re-purposed 4-cycle internal combustion engine. Inert gas and a small volume-fraction of pulverized biomass are input into the RBCR intake, and the crankshaft is cycled by an external energy source to supply the process heat. The biomass is converted during the compression stroke, and then the bio-products are exhausted. The cycle is: intake, compression/heating, expansion, and exhaust. A control-volume energy balance to assess the steady-state flow of mass and energy through the RBCR is presented. The RBCR calculations are quantitatively compared to experimental results from the state of the art considered to be a lab-scale fluidized-bed reactor (FBR) found in the literature. This FBR is chosen for comparison because the RBCR and FBR have nearly the same size/footprint and, thus, by crude assumption, similar capital costs. Relative to the state-of-the-art (SOA), calculations predict that the RBCR will increase the biomass throughput, decrease the mass-specific energy requirement to thermochemically convert biomass to bio-oil, bio-char, and bio-gas by fast-pyrolysis. Moreover, calculations predict that at bench scale, the RBCR process results in a bio-oil product with a heating value approximately 6.8 times higher than the energy required to drive the cycle (there is a 6.8 times "return on energy investment").

1. Introduction

Fast pyrolysis is a process where biomass is decomposed in an environment without an oxidizing agent at temperatures of approximately 500 °C for short times. Thermochemical biomass conversion by fast pyrolysis to bio-oil, bio-char, and bio-gas is a part of an attractive path to an alternative energy source because of the upgrade in heating value and density [1] so that it may be easily transported as part of a new distribution network [2,3]. Effective methods of biomass conversion to bio-oil are of interest because bio-oil represents a deployable energy carrier with favorable source characteristics (e.g., in-situ production and carbon-neutral) [4–9]. Biomass is pulverized, pyrolyzed, and the bio-products are recovered (Fig. 1). Bio-oil can be used directly in boilers (i.e., for heating or electricity), or upgraded for use as a fuel [2].

There are a number of reactor types for fast pyrolysis: entrained flow reactor, wire mesh reactor, vacuum furnace reactor, vortex reactor, rotating reactor, microwave reactor, fluidized-bed reactor, and the circulating fluidized-bed reactor [10–20]. The fluidized-bed reactor (FBR) is representative of the current state of the art. In an FBR, primary pyrolysis reactions of the biomass lead to pyrolysis vapor which can be condensed to bio-oil, which is ultimately the desired product of the fast-pyrolysis process. Following the primary pyrolysis reactions, secondary pyrolysis reactions can occur which adversely affect the bio-oil quality and should be avoided [1,10,12,16,21]. The FBR requires a condenser to cool the bio-products to quench the secondary pyrolysis reactions and condense the bio-oil for collection [16]. The condenser in an FBR is an active cooling component that leads to heat loss and system inefficiency.

In this work, we describe a novel reactor for the conversion of biomass that can reduce energy requirements and rapidly quench unwanted secondary pyrolysis reactions. It is termed the 'reciprocating biomass conversion reactor' (RBCR). At its essence, the conversion scheme is a high compression-ratio motor being cycled by an external power source to efficiently provide process heat to biomass. A model is presented for the decomposition of multi-component biomass in an RBCR. Specifically, bagasse decomposition for the compression and expansion strokes of the RBCR is described. Additionally, a sensitivity study is presented by fixing all but one parameter, namely: engine speed, biomass particle diameter, biomass feed-rate, and biomass composition.

E-mail address: nick.parziale@gmail.com (N.J. Parziale)

https://doi.org/10.1016/j.ijheatmasstransfer.2019.118988
0017-9310/

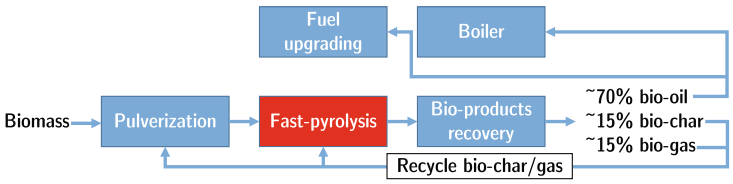

Fig. 1. Flow chart for thermochemical conversion of biomass by fast pyrolysis. Biomass is pulverized, pyrolyzed, and the bio-oil is recovered for use in a boiler (directly for heat or electricity), or upgraded for use as bio-diesel or aviation fuel [2]. The bio-char and bio-gas can be recycled for use as an energy source for the required energy for pulverization and fast-pyrolysis. The approximate fractions of bio-products are taken from the literature [10]. The contribution of this paper is to predict the performance of a novel means to thermochemically convert biomass by. fast pyrolysis.

2. Reciprocating biomass conversion reactor (RBCR) cycle

The reciprocating biomass conversion reactor (RBCR) cycle utilizes rapid heating/conversion and cooling of a small volume-fraction of pulverized biomass suspended in a non-oxidizing gas within a cylinder [22,23]. The process flowchart is presented as Fig. 2. In a typical Diesel engine, the 4-stroke cycle is: intake, compression, power, and exhaust; in the proposed conversion scheme, this is replaced with: intake, compression/heating, expansion, and exhaust. The idealized cycle for the proposed biomass conversion scheme proceeds as follows:

1. *Intake:* A two-phase mixture of inert fluidizing gas (Ar, N_2, or a CO/CO_2 mixture) and a small volume-fraction of pulverized biomass are input into the cylinder of a high compression ratio engine.
2. *Compression/heating:* An external power source (e.g., an electric motor) turns the crankshaft driving the piston to compress and heat the biomass/ fluidizing-gas mixture within the cylinder. Process heat is transferred from the fluidizing gas to the biomass, primarily by convection; this process heat is sufficient to thermochemically convert the biomass to bio-products by fast pyrolysis.
3. *Expansion/cooling:* The expansion stroke rapidly decreases the temperature and pressure of the fluidizing-gas/ bio-products mixture within the cylinder, quenching the undesirable secondary pyrolysis reactions, and condensing the bio-oil to finely atomized droplets. A significant fraction of the energy required to compress the system is recovered as the pressure is reduced through expansion. The recovered energy may be used on the compression stroke of another cylinder on the same crankshaft.
4. *Exhaust:* The exhaust stroke forces the fluidizing-gas/ bio-products mixture from the cylinder. The bio-products are collected, and the fluidizing gas is collected and recycled.

This cycle has the potential to reduce operating costs of thermochemical conversion by reducing the required input energy to the system and improving the quality of the bio-products by quenching undesirable secondary pyrolysis reactions. The instant following desired biomass conversion, the bio-products, and fluidizing gas reside within the cylinder at an elevated temperature and pressure. This is surplus process heat, and in contrast to the state of the art, the surplus process heat is transferred and reused mechanically through the crankshaft to another piston/cylinder during the expansion stroke. In the following sections, we present a model to predict the useful biomass conversion parameter space of the RBCR.

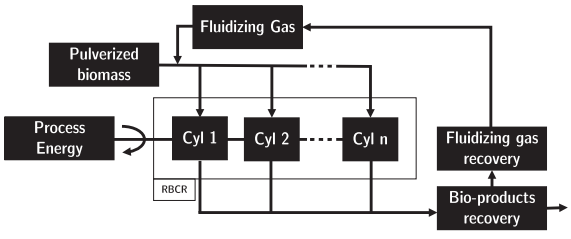

Fig. 2. Reciprocating biomass conversion reactor (RBCR) process flowchart.

3. Closed control-volume energy balance

Here, we analyze a closed control volume, presented as Fig. 3, which surrounds one cylinder of the RBCR shown in Fig. 2. There is a well-mixed and evenly distributed fluidizing gas and biomass/bio-products mixture in this control volume; the fluidizing gas and biomass are separated in Fig. 3 only to clearly show the direction of energy transfer. In Fig. 3, Q is the energy that is transferred into the control volume by heat transfer, W is the energy that is transferred out of the control volume by work, and ΔH_P is the change in enthalpy required to pyrolyze the biomass. The subscripts b, g, and w represent the biomass, fluidizing gas, and wall, respectively. Two subscripts in succession indicate "from a to b," e.g., Q_{gb} is the energy transferred from the fluidizing gas to the biomass by heat transfer. Additionally, we assume that the pressure of the fluidizing gas and biomass are equal, $P_g = P_b = P$.

The change in internal energy for the fluidizing gas is $\Delta U_g = c_{vg} n_g \Delta T_g$ and the work term is $W_{gw} = P\Delta V_g$. Here, $c_{vg}, n_g, \Delta T_g$, and V_g are the constant-volume molar specific heat, number of moles, change in temperature, and volume of the fluidizing gas, respectively. The first law for the control volume of the fluidzing-gas is written as

$$\begin{aligned} \Delta U_g &= Q_g - W_g = -Q_{gb} + Q_{wg} - W_{gw} \\ \Delta U_g &= c_{vg} n_g \Delta T_g = -Q_{gb} + Q_{wg} - P\Delta V_g. \end{aligned} \tag{1}$$

The change in enthalpy of the biomass, ΔH_b, includes the change in sensible enthalpy, ΔH_S, and the enthalpy of pyrolysis reactions, ΔH_P, as $\Delta H_b = \Delta H_S + \Delta H_P = \Delta U_b + \Delta(PV_b)$. We assume that there is no volumetric change of the biomass. The change in enthalpy due to pyrolysis is $\Delta H_P = m_P \Delta h_P$, and the change in sensible enthalpy is

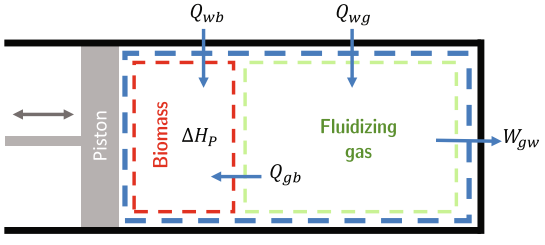

Fig. 3. Control volume for analysis of the compression and expansion strokes of the RBCR. The red marks the control volume for the biomass, the green marks the control volume for the fluidizing gas, and the blue marks the control volume enclosing the cylinder for one cycle. We assume a well-mixed and evenly distributed fluidizing gas and biomass/bio-products mixture in this control volume; they are separated only to clearly show the direction of energy transfer.

Please cite this article as: N. J. Parziale and R. Adhikari, Model and sensitivity analysis of the reciprocating biomass conversion reactor (RBCR), International Journal of Heat and Mass Transfer, https://doi.org/10.1016/j.ijheatmasstransfer.2019.118988

$\Delta H_S = m_b c_b \Delta T_b$. Here $m_p, \Delta h_P, m_b, c_b$, and ΔT_b are the pyrolyzed mass, mass-specific enthalpy of pyrolysis, biomass mass, biomass mass-specific heat, and change in biomass temperature, respectively. The first law for the control volume for the biomass is written as

$$\begin{aligned} \Delta U_b &= Q_b - W_b = Q_{gb} + Q_{wb} - W_b \\ \Delta U_b &= m_b c_b \Delta T_b + m_P \Delta h_P - V_b \Delta P = Q_{gb} + Q_{wb} \end{aligned} \tag{2}$$

4. Transient RBCR Control Volume

A more detailed treatment will be presented in this section to predict the transient response of the RBCR. Differential equations are formulated from the application of the first law to the fluidizing gas and the biomass/bio-products in the reactor (Eqs. (1) and (2)). The time-rate form of Eq. (1) is

$$\frac{dT_g}{dt} = \left(-\dot{Q}_{gb} + \dot{Q}_{wg} - P\frac{dV_g}{dt} \right) / (c_{vg} n_g). \tag{3}$$

Inspection of Eq. (3) implies that the time-rate of change of temperature is increased by cylinder volume decrease and decreased by heat transfer to the surroundings. The dV_g/dt term is prescribed by considering the kinematic motion of the piston [24]. The evolution of bio-products are predicted by coupling the above control-volume energy balance with a biomass decomposition mechanism. The biomass is assumed to be a collection of independent spheres that act as a lumped mass, m_b, with specific heat c_b, and a constant volume. Individual fractions of m_b are permitted to evolve as computed by the first-order kinetics mechanism reviewed in Xue et al. [25] (Fig. 4). Additionally, the rate of energy loss due to pyrolysis, $\dot{Q}_{\Delta h}$, is included in the calculations. Because the collection of independent spheres act as a lumped mass, Eq. (2) can be rewritten to predict the biomass temperature (T_b) change as

$$\frac{dT_b}{dt} = \left(\dot{Q}_{gb} + \dot{Q}_{wb} - \Delta \dot{H}_P + V_b \frac{dP}{dt} \right) / (m_b c_b). \tag{4}$$

The dP/dt term can be related to the time rate of change of the fluidizing-gas temperature and volume change through the differentiation of the logarithm of the ideal gas law as

$$\frac{dP}{dt} = P\left(\frac{1}{T_g}\frac{dT_g}{dt} - \frac{1}{V_g}\frac{dV_g}{dt} \right). \tag{5}$$

The emerging nature of the biomass pyrolysis modeling field (reviews in [18,26–28]) presents a number of options to model the production rates of bio-products. We choose a model which "superposes" cellulose, hemicellulose, and lignin as

$$m_b = m_c + m_h + m_l, \tag{6}$$

where m_c, m_h, and m_l are the individual masses of cellulose, hemicellulose, and lignin, respectively. The fractions of the biomass are defined as $\alpha = m_c/m_b, \beta = m_h/m_b$, and $\gamma = m_l/m_b$. The evolution of these fractions are modeled simultaneously and independently. Examples of different compositions are given in Table 1.

The mechanism to predict the decomposition of biomass closely follows the development in references [25,29–40]. In particular, the works by Xue et al. [25,40] have resulted in a model which will be used for this work. We use the model by Xue et al. because it is relatively simple to implement, and was demonstrated to have reasonable agreement with experimental data for fast pyrolysis in [40]. Additionally, this model is able to handle the parallel reactions of cellulose, hemicellulose, and lignin, and also considers the competitive reactions of active biomass decomposing to tar vapor or char and gas, and the secondary decomposition of tar vapor to gas. The mechanism appears as Fig. 4, and pictorially depicts how the cellulose, hemicellulose, and lignin decompose. The indices for each component can be found in Table 2. The rates of change for the masses are written as

$$\dot{m}_1 = -k_{1C} m_1 \tag{7a}$$
$$\dot{m}_2 = -k_{1H} m_2 \tag{7b}$$
$$\dot{m}_3 = -k_{1L} m_3 \tag{7c}$$
$$\dot{m}_4 = k_{1C} m_1 - k_{2C} m_4 - k_{3C} m_4 \tag{7d}$$
$$\dot{m}_5 = k_{1H} m_2 - k_{2H} m_5 - k_{3H} m_5 \tag{7e}$$
$$\dot{m}_6 = k_{1L} m_3 - k_{2L} m_6 - k_{3L} m_6 \tag{7f}$$
$$\dot{m}_7 = k_{2C} m_4 + k_{2H} m_5 + k_{2L} m_6 - k_4 m_7 \tag{7g}$$
$$\dot{m}_8 = (1 - Y_C) k_{3C} m_4 + (1 - Y_H) k_{3H} m_H + (1 - Y_L) k_{3L} m_6 - \Gamma \tag{7h}$$
$$\dot{m}_9 = Y_C k_{3C} m_4 + Y_H k_{3H} m_H + Y_L k_{3L} m_6 + \Gamma, \tag{7i}$$

where gamma is the rate at which char is formed in the pores in the biomass, per Xue et al. [25,40],

$$\Gamma = \frac{\rho_g}{\rho_b}(\dot{m}_1 + \dot{m}_2 + \dot{m}_3 + \dot{m}_4 + \dot{m}_5 + \dot{m}_6) - \frac{\rho_g}{\rho_c}\dot{m}_9. \tag{8}$$

The first-order kinetic rates of Arrhenius form, $k_i = A_i \exp(E_i/(R_u T_b))$, are tabulated for each component in Table 3, and R_u is the universal gas constant. The char formations ratios are $Y_C = 0.35, Y_H = 0.60$, and $Y_L = 0.75$, for cellulose, hemicellulose, and lignin, respectively [25,29,30,34].

The time-rate-of-change of the enthalpy change for the conversion processes in Fig. 4 is $\Delta \dot{H}_P$ in Eq. (4). This value is calculated as

$$\Delta \dot{H}_P = \Delta \dot{H}_{\Delta htf} + \Delta \dot{H}_{\Delta gf} + \Delta \dot{H}_{\Delta cf} \tag{9a}$$
$$\Delta \dot{H}_{\Delta htf} = \Delta h_{tf}(k_{2C} m_4 + k_{2H} m_5 + k_{2L} m_6) \tag{9b}$$
$$\Delta \dot{H}_{\Delta hgf} = \Delta h_{gf} \dot{m}_8 \tag{9c}$$
$$\Delta \dot{H}_{\Delta hcf} = \Delta h_{cf} \dot{m}_9 \tag{9d}$$

Table 1
Biomass composition fraction from [29].

Feedstock	Cellulose	Hemicellulose	Lignin
Pure Cellulose	1.00	0.00	0.00
Bagasse	0.36	0.47	0.17
Oak	0.35	0.40	0.25
Olive Husk	0.22	0.33	0.45

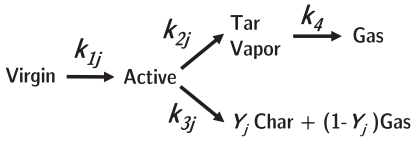

Fig. 4. Mechanism for pyrolysis adapted from [25,29–40]. j may be cellulose C, hemicellulose H, or .lignin, L.

Table 2
Indices of each component.

Component	Index
Virgin Cellulose	1
Virgin Hemicellulose	2
Virgin Lignin	3
Active Cellulose	4
Active Hemicellulose	5
Active Lignin	6
Tar Vapor	7
Gas	8
Char	9

Please cite this article as: N. J. Parziale and R. Adhikari, Model and sensitivity analysis of the reciprocating biomass conversion reactor (RBCR), International Journal of Heat and Mass Transfer, https://doi.org/10.1016/j.ijheatmasstransfer.2019.118988

Table 3
Kinetics data.

Rate Constant	A (1/s)	E (MJ/kmol)	Reference
k_{1C}	2.80e19	242.4	[25,30]
k_{2C}	3.28e14	196.5	[25,30]
k_{3C}	1.30e10	150.5	[25,30]
k_{1H}	2.10e16	186.7	[25,29]
k_{2H}	8.75e15	202.4	[25,29]
k_{3H}	2.60e11	145.7	[25,29]
k_{1L}	9.60e8	107.6	[25,29]
k_{2L}	1.50e9	143.8	[25,29]
k_{3L}	7.70e6	111.4	[25,29]
k_4	4.25e6	108.0	[25,34]

where $\Delta h_{tf} = -255$ kJ/kg [37], $\Delta h_{gf} = 20$ kJ/kg [37], and $\Delta h_{cf} = 42$ kJ/kg [35] are the heats of reaction for tar, gas, and tar formation respectively. A negative sign indicates an endothermic reaction.

The combined natural/forced heat transfer coefficients are found from correlations [41]. The convection to the walls [42] and to the biomass [43] are assumed to be steady by non-dimensional analysis. Mass transfer will reduce the heat transfer coefficient to the biomass, so the high mass-transfer rate film theory correction [44,45] is used as

$$\frac{h^*}{h} = \frac{\phi_T}{\exp(\phi_T) - 1}. \tag{10}$$

Here, h^* and h are the corrected and uncorrected heat transfer coefficients, respectively, and ϕ_T is defined as

$$\phi_T = \frac{\dot{m}_\phi c_{tv}}{A_s h}. \tag{11}$$

Here, c_{tv} is the specific heat of the tar vapor, and A_s is the surface area of the biomass particle. The mass loss from the biomass particle that is considered to reduce the heat transfer coefficient is $\dot{m}_\phi$ and may be written as

$$\dot{m}_\phi = k_{2C}m_4 + k_{2H}m_5 + k_{2L}m_6 + (1 - Y_C)k_{3C}m_4 + (1 - Y_H)k_{3H}m_H + (1 - Y_L)k_{3L}m_6 \tag{12}$$

Thermophysical properties for the fluidizing gas are calculated using Cantera [46] with the appropriate thermodynamic data [47] fitted to polynomials of temperature. The cylinder wall emissivity ($\epsilon_w = 0.05$) is taken to be that of polished steel [48]. The biomass true density is assumed to be that of cellulose: $\rho_b = 1580$ kg/m^3 [49]. The specific heat of the biomass (c_b) is assumed to be that of cellulose

$$c_b = c_{gluc}(A + T_b B) \tag{13}$$

where $A = 0.9830$ J/mol-K and $B = 3.963\text{e}{-4}$ J/mol-K^2. The vibrational contribution to the heat capacity of glucose can be written as

$$c_{gluc} = \sum_i R_u \left(\frac{h\nu_i}{kT_b}\right)^2 \exp\left(\frac{h\nu_i}{kT_b}\right)\left(\exp\left(\frac{h\nu_i}{kT_b}\right) - 1\right)^{-2} \tag{14}$$

where R is the universal gas constant, h is Planck's constant, k is Boltzmann's constant, and ν_i is a frequency of the ith normal vibration [50].

Eqs. (3), (4), and (7) are implicit ordinary differential equations that are integrated in time to calculate the evolution of pressure, biomass temperature, fluidizing gas temperature, and conversion fractions for the compression and expansion strokes of the RBCR. The initial conditions are:

- The biomass begins as virgin material (Fig. 4).
- The initial biomass and fluidizing gas temperatures are $T_b = T_g = 22\ ^\circ$C.
- The mass of the biomass m_b and the biomass radius r_b are specified for one cycle.

MATLAB [51] is used to perform the integration for the implicit equations for the prescribed cycle period which is determined by the engine speed; the results for the integrations presented herein are not sensitive to the ODE solver tolerance, bringing confidence in the calculation result.

5. Results of bagasse conversion calculations in an RBCR

In this section, we apply the model described in Section 4 to the decomposition of bagasse in an RBCR. The core of the reactor is assumed to be an 8-cylinder, 4-stroke, 7.3 L Diesel motor with a compression ratio of 21.5, modeled after the ubiquitous Ford 7.3 L Powerstroke Diesel Engine. A mixture of argon and spherical biomass particles 50 μm in diameter is injected into the intake of the engine. Argon is chosen as the fluidizing gas over alternatives such as N_2 because argon has a higher ratio of specific heats and a lower constant-volume specific heat. As a result, the increase in the temperature (thermal energy) of the fluidizing gas is larger when using argon than when using nitrogen (see Eq. (3)), and a higher amount of energy is then available for heat transfer to biomass for conversion. The composition of the biomass is split between cellulose, hemicellulose, and lignin to simulate bagasse decomposition (Table 1). The thermophysical properties of the biomass are assumed to be those of cellulose, per the discussion in Section 4.

Parameters and results for the decomposition of bagasse are given in Table 4. Tabulated are: the number of cylinders, bore, stroke, engine speed, mass flow of fluidizing gas $\dot{m}_{FG}$, volume-fraction of biomass V_F, the input energy per unit mass of biomass required to thermochemically convert the biomass e_{in}, and the feed rate of biomass $\dot{m}_b$.

A figure of merit, termed 'return on energy investment,' is the ratio of power available from bio-oil out to the power required to operate the reactor, η, is written as

$$\eta = \frac{\dot{m}_b Q_{hv} Y_{tv/bo}}{\dot{Q}_{in}}, \tag{15}$$

where $Q_{hv} \approx 20$ MJ/kg is the heating value of bio-oil [52], $Y_{tv/bo}$ is the mass fraction of tar vapor or bio-oil for the calculations and the experimental results, respectively. The power supplied to the reactor is

$$\dot{Q}_{in} = \int_{\text{cycle}} pdV/t_{cycle} + \dot{m}_b e_{\text{comminute}}, \tag{16}$$

where the pressure-volume work per-unit cycle and power required to comminute the biomass to 50 μm are included. We conservatively estimate $e_{\text{comminute}} \approx 1$ MJ/kg by extrapolating from the values given in Mani et al. [53].

Table 4
Comparison of calculated RBCR results with experimental lab-scale fluidized-bed reactor results.

Parameter	RBCR	Lab FBR [21]
Cylinders	8	–
Bore	104 mm	–
Stroke	106 mm	–
RPM	200	–
$\dot{m}_{FG/CG}$	75 kg/hr (Ar)	4.8 kg/hr (N_2)
V_F	74 ppm	0.46 (wt/wt)
$\dot{m}_b$	5.3 kg/hr	2.2 kg/hr
Feedstock	Bagasse	Switchgrass
e_{in}	2.1 MJ/kg	3.5 MJ/kg
η	6.8	3.5
Input particle diameter	50 μm	<500 μm

Please cite this article as: N. J. Parziale and R. Adhikari, Model and sensitivity analysis of the reciprocating biomass conversion reactor (RBCR), International Journal of Heat and Mass Transfer, https://doi.org/10.1016/j.ijheatmasstransfer.2019.118988

Experimental results from a lab-scale fluidized bed reactor (Lab FBR) are taken from the literature [21] for the purposes of comparison because the RBCR and FBR have nearly the same size/footprint and, thus, by crude assumption, similar capital costs. For context, the reactor volume in the RBCR consists of 8 cylinders each with a bore of 104 mm and a stroke length of 106 mm. The FBR has a single reactor vessel of 78 mm diameter and 520 mm length. In addition, the FBR has four condensers each with a size of 100 mm $\times$ 200 mm. In the RBCR, the biomass and the bio-products reside in a cylinder for 300 ms. During this period, the biomass is pyrolyzed and the bio-products are cooled to temperatures that cause the bio-oil to condense in the form of fine mist. For the FBR, the residence time in the reactor is 650 ms, followed by a relatively long period to cool the bio-products in the condensers.

A time-history of reactor pressure P, fluidizing gas temperature T_g, and biomass temperature T_b for the reactor is presented as Fig. 5 for the compression and expansion strokes of the RBCR cycle. The maximum temperature of the biomass is over 500 °C and the heating rate exceeds 5000 °C/s during the compression stroke; these temperatures and heating rates are consistent with those found in the literature for fast pyrolysis [16]. The bio-products are rapidly cooled at over −5000 °C/s during the expansion stroke; the rapid bio-product cooling will quench the undesirable secondary pyrolysis reactions. That is, the undesirable conversion from tar vapor to gas/char can be quenched (see Fig. 4). For context, Boateng et al. [21] report −60 °C/s cooling in a bench-scale fluidized bed reactor with condensers packed with dry ice.

In Fig. 6, the biomass weight fraction evolution is presented per the model formulated in Section 4. The virgin/active cellulose and hemicellulose are degraded primarily between 0.10 and 0.20 s. The virgin lignin is degraded completely; however, there is still active lignin in the output of the reactor at this condition. This is unconverted biomass. At the end of an expansion stroke, ≈70% of the biomass is converted to pyrolysis vapor. Little undesirable secondary gas and char are produced because the rapid expansion stroke quenches all reactions within the cylinder.

The disparity between the fluidizing gas temperature (green) and the biomass temperature (red) in Fig. 5 occurs between 0.10 and 0.20 s; the increase in biomass temperature appears to be stunted. It is during this time that the biomass is undergoing conversion (Fig. 6). Per the formulation in Section 4, the conversion process impedes heating because conversion to tar vapor is endothermic (per Eqs. (4) and (9b)) and the heat transfer coefficient is reduced by film cooling (per Eqs. (10) and (11)).

6. Results of sensitivity study

In this section, we report the results of a sensitivity study that was performed by fixing all but one parameter, namely engine speed, biomass particle diameter, biomass feed-rate, and biomass composition. The parameters and initial conditions are the same as in Section 5 and Table 4. The purpose of this exercise was to investigate how sensitive the RBCR concept is to variations in input conditions and to aid in defining an intelligent operating parameter space.

In Fig. 7, the rotational speed is varied as all other parameters are fixed. The figure aids in defining the operating speed for the RBCR. Near-complete conversion is calculated to occur for rotational speeds of 20–100 RPM, otherwise, there is non-converted

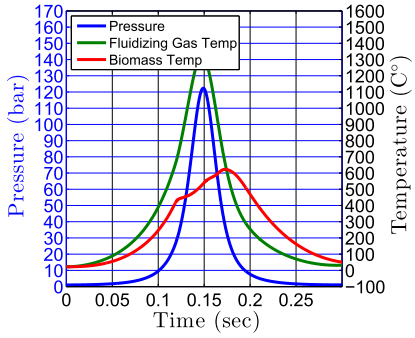

Fig. 5. Calculation of compression (0–0.15 s) and expansion (0.15–0.30 s) strokes for the pilot-scale experiment. Calculation of reactor pressure P (blue), fluidizing gas temperature T_g in (green), and biomass temperature T_b (red).

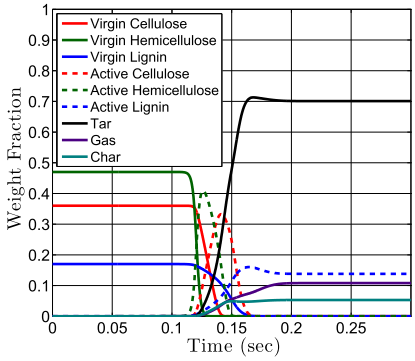

Fig. 6. Calculation of compression (0–0.075 s) and expansion (0.075–0.130 s) strokes for the pilot-scale experiment. Calculated weight fractions vs. time per the model formulated in Section 4.

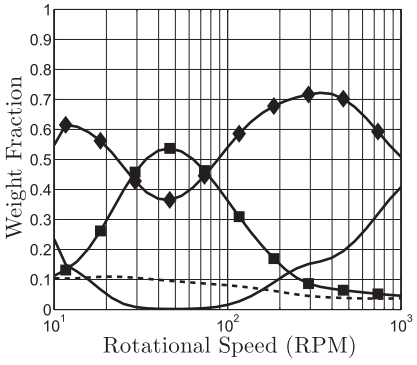

Fig. 7. Calculation of weight fraction as a function of engine speed. Conversion fractions of tar vapor (◆ markers), gas (■ markers), char (no markers, dashed), and non-converted biomass (remaining virgin and active cellulose, hemicellulose, and lignin – no markers).

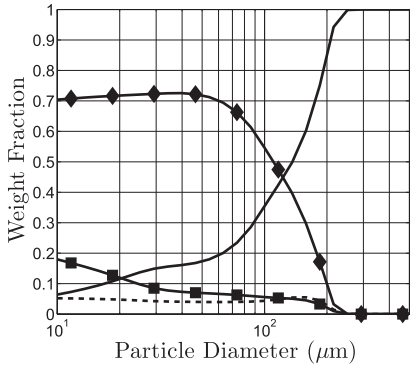

Fig. 8. Calculation of conversion fraction as a function of particle diameter. Conversion fractions of tar vapor (◆ markers), gas (■ markers), char (no markers, dashed), and non-converted biomass (remaining virgin and active cellulose, hemicellulose, and lignin – no markers).

Please cite this article as: N. J. Parziale and R. Adhikari, Model and sensitivity analysis of the reciprocating biomass conversion reactor (RBCR), International Journal of Heat and Mass Transfer, https://doi.org/10.1016/j.ijheatmasstransfer.2019.118988

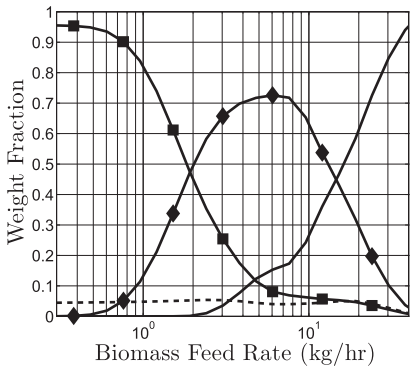

Fig. 9. Calculation of conversion fraction as a function of biomass feed-rate. Conversion fractions of tar vapor (◆ markers), gas (■ markers), char (no markers, dashed), and non-converted biomass (remaining virgin and active cellulose, hemicellulose, and lignin - no markers).

biomass within the cylinder after one cycle. The lower limit, 20 RPM, is a result of the higher fraction of input energy lost to heat transfer to the cylinder walls; that is, the compression stroke is highly non-adiabatic, and thus less energy is available for conversion. For engine speeds higher than 100 RPM, complete conversion cannot occur because of kinetic and heat transfer limitations. If the goal is to maximize the conversion of biomass to bio-oil, an engine speed of 200–500 RPM is appropriate to increase the yield of tar vapor and maximize the throughput of the RBCR.

In Fig. 8, the biomass particle diameter is varied while all other parameters are held fixed. Calculations indicate that conversion decreases with increasing biomass diameter. The capability for the RBCR to convert biomass is reduced at a particle diameter of greater than 150 μm. Additionally, it appears that the fraction of bio-gas is increased below 150 μm. The surface area available for heat transfer scales inversely with particle diameter. This inverse scaling overcomes the scaling of the heat transfer coefficient with diameter. So, heat transfer to the biomass particle is calculated to be more efficient at smaller diameters, and this is the reason for the trends that appear in Fig. 8.

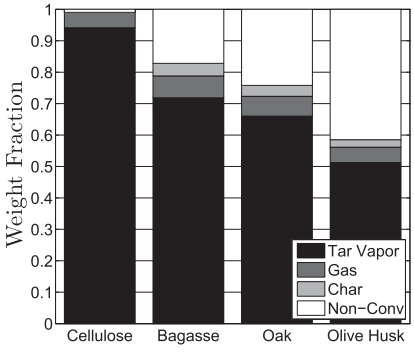

Fig. 10. Calculation of conversion fractions of tar vapor, gas, char, and non-converted biomass. Mechanism shown in Fig. 4, and biomass compositions given in Table 1.

In Fig. 9, the biomass feed-rate is varied as the other parameters are held fixed. Calculations predict that complete conversion occurs for biomass feed-rates of less than 2 kg/hr. Decreasing the feed-rate far below 1 kg/hr is predicted to result in large fractions of bio-gas at the expense of tar vapor production. If the goal of the RBCR is to maximize bio-oil yield, the operational limit for biomass feed-rate would be 3–10 kh/hr to maximize the tar vapor yield. For this scale of RBCR, there is significant unconverted biomass at mass feed-rates of higher than 10 kg/hr.

In Fig. 10, the biomass composition fraction is varied. The initial composition is superimposed per Eq. (6). Pure cellulose, bagasse, oak, and olive husk are considered. The feedstocks are chosen because of the increasing lignin content (see Table 1). Lignin is generally understood to make bio-oil production more difficult [1,16]. It is calculated that cellulose is completely converted. The other feedstocks are not completely converted and the tar vapor weight fraction is reduced.

7. Preliminary results and practical considerations

Currently, we are constructing an apparatus testbed as shown in Fig. 11(left). With this setup, we have the proper infrastructure in place to perform detailed performance tests of the proposed concept. To date, we have devised a biomass injection apparatus with sufficient metering control and performed preliminary conversion tests using argon as the fluidizing gas and 20 μm cellulose purchased from Sigma Aldrich as the feedstock. In Fig. 11(right), we show the mist formed by the bio-products at the RBCR outlet which represents the first successful conversion of biomass with the RBCR. In the future, we plan to capture the bio-char with a cyclone or impingement style separator followed by an electrostatic precipitator to capture the bio-oil, following the methods found in Perry and Chilton [54,55]. We recognize that appropriate separation of the different bio-products will be an appreciable practical consideration moving forward.

An additional practical consideration would be the so-called tarring of the reactor by deposition of the condensed liquid and solid particulates on the reactor walls during long periods of operation. Our short (10 min) preliminary experiments indicate, qualitatively, that this is not an issue. But, we will quantify the possible run times before reactor tarring becomes an issue, if ever. Moreover, we have strategies to treat reactor tarring should it be found to compromise performance. If we were to notice tarring becoming an issue, we can attempt to remove the deposits by a) running the

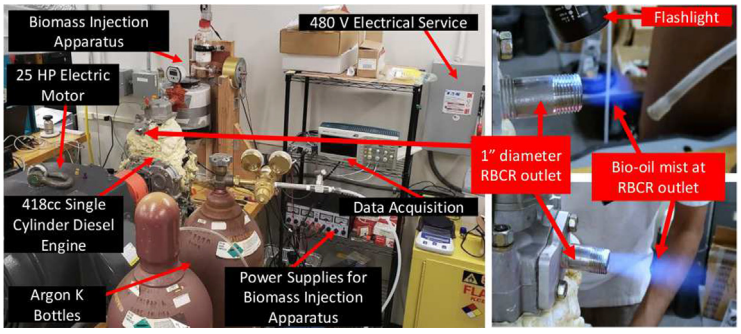

Fig. 11. RBCR setup at the Stevens Institute of Technology. Right: Preliminary results of bio-oil mist being produced in RBCR.

Please cite this article as: N. J. Parziale and R. Adhikari, Model and sensitivity analysis of the reciprocating biomass conversion reactor (RBCR), International Journal of Heat and Mass Transfer, https://doi.org/10.1016/j.ijheatmasstransfer.2019.118988

RBCR with a fuel/air mixture or, b) running steam through the reactor.

8. Summary and conclusion

In this paper, a model is formulated for the decomposition of multi-component biomass in a reciprocating biomass conversion reactor (RBCR). A description of the decomposition of bagasse is presented for the compression and expansion strokes of the RBCR. Additionally, a sensitivity study was presented by fixing all but one parameter, namely: engine speed, biomass particle diameter, biomass feed-rate, and biomass composition.

The RBCR decomposition of bagasse calculations compare favorably to the experimental data for a lab-scale fluidized bed reaction. This FBR was chosen because the RBCR and FBR have nearly the same size/footprint and, thus, by crude assumption, similar capital costs. Calculations indicate that the efficiency and 'return on energy investment' is increased by greater than ≈50%. The throughput also compares favorably to the FBR, as the RBCR is able to process significantly more biomass. Such efficiency and throughput increases would result in a decrease in the operational costs of biomass conversion. The RBCR permits control over the residence time within the reactor so that unwanted secondary pyrolysis reactions will not take place. This is because immediately following thermochemical conversion, the bio-products and fluidizing gas are rapidly cooled during the expansion stroke, and the secondary pyrolysis reactions are rapidly quenched. This process is in direct contrast to the FBR where the pyrolysis products must be processed by condensers to quench the unwanted secondary reactions; this process requires a longer time to undergo and there is additional heat loss.

The sensitivity study of the RBCR to input parameters indicates that the reactor is flexible in what it is able to accomplish. Preferential bio-gas or bio-oil production may be accomplished by adjusting the biomass feed-rate and engine speed. Engine speed and biomass feed-rate are easily controlled relative to the calculated sensitivities.

The most significant limitation of this reactor is the sensitivity to particle size. Calculations predict that there will be a significant fraction of unconverted biomass for particle sizes of greater than 200 μm. This size restriction poses an operational constraint as well as an additional overall energy input requirement to the conversion setup; although, even with this additional energy required for biomass pulverization, the RBCR compares favorably to the FBR.

Bagasse, oak, and olive husk were considered as candidates for RBCR feed-stock. It appears that bagasse is a strong candidate because of its lower lignin content. The lower lignin content is possibly more important in the RBCR because of the shorter residence time than typically encountered in FBRs. Pure cellulose could be used as the feed-stock for RBCR development because it is easier to completely convert.

Declaration of Competing Interest

The authors declare that they have no known competing financial interests or personal relationships that could have appeared to influence the work reported in this paper..

Acknowledgments

Stevens Institute of Technology supported this work. We would also like to thank Prof. R. Besser for his helpful and insightful comments. The authors are also grateful for support from the PSEG Foundation to advance energy innovation at Stevens Institute of Technology.

Appendix A. Supplementary material

Supplementary data associated with this article can be found, in the online version, at https://doi.org/10.1016/j.ijheatmasstransfer.2019.118988.

References

[1] D. Mohan, C.U. Pittman, P.H. Steele, Pyrolysis of wood/biomass for bio-oil: a critical review, Energy Fuels 20 (3) (2006) 848–889, https://doi.org/10.1021/ef0502397.
[2] M. Wright, R.C. Brown, Establishing the optimal sizes of different kinds of biorefineries, Biofuels, Bioprod. Biorefin. 1 (3) (2007) 191–200, https://doi.org/10.1002/bbb.25.
[3] M. Wright, R.C. Brown, A.A. Boateng, Distributed processing of biomass to bio-oil for subsequent production of fischer-tropsch liquids, Biofuels, Bioprod. Biorefin. 2 (3) (2008) 229–238, https://doi.org/10.1002/bbb.73.
[4] J. Lehmann, J. Gaunt, M. Rondon, Bio-char sequestration in terrestrial ecosystems – a review, Mitig. Adapt. Strat. Glob. Change 11 (2) (2006) 395–419, https://doi.org/10.1007/s11027-005-9006-5.
[5] J. Lehmann, A handful of carbon, Nature 447 (7141) (2007) 143–144, https://doi.org/10.1038/447143a.
[6] D.A. Laird, The charcoal vision: a win–win–win scenario for simultaneously producing bioenergy, permanently sequestering carbon, while improving soil and water quality, Agron. J. 100 (1) (2008) 178–181, https://doi.org/10.2134/agrojnl2007.0161.
[7] D.A. Laird, R.C. Brown, J.E. Amonette, J. Lehmann, Review of the pyrolysis platform for coproducing bio-oil and biochar, Biofuels, Bioprod. Biorefin. 3 (5) (2009) 547–562, https://doi.org/10.1002/bbb.169.
[8] J.W. Lee, B. Hawkins, D.M. Day, D.C. Reicosky, Sustainability: the capacity of smokeless biomass pyrolysis for energy production, global carbon capture and sequestration, Energy Environ. Sci. 3 (11) (2010) 1695–1705, https://doi.org/10.1039/C004561F.
[9] D. Woolf, J.E. Amonette, F.A. Street-Perrott, J. Lehmann, S. Joseph, Sustainable biochar to mitigate global climate change, Nat. Commun. 1 (2010) 56, https://doi.org/10.1038/ncomms1053.
[10] R.C. Brown, Biochar production technology, in: J. Lehmann, S. Joseph (Eds.), Biochar for Environmental Management: Science and Technology, Earthscan, 2009.
[11] B. Krieger-Brockett, Microwave pyrolysis of biomass, Res. Chem. Intermed. 20 (1) (1994) 39–49, https://doi.org/10.1163/156856794X00054.
[12] D. Meier, O. Faix, State of the art of applied fast pyrolysis of lignocellulosic materials – a review, Bioresour. Technol. 68 (1) (1999) 71–77, https://doi.org/10.1016/S0960-8524(98)00086-8.
[13] S. Czernik, A.V. Bridgwater, Overview of applications of biomass fast pyrolysis oil, Energy Fuels 18 (2) (2004) 590–598, https://doi.org/10.1021/ef034067u.
[14] A.V. Bridgwater, D. Meierb, D. Radlein, An overview of fast pyrolysis of biomass, Org. Geochem. 30 (1999) 1479–1493, https://doi.org/10.1016/S0146-6380(99)00120-5.
[15] A.V. Bridgwater, G.V.C. Peacocke, Fast pyrolysis processes for biomass, Renew. Sustain. Energy Rev. 4 (1) (2000) 1–73, https://doi.org/10.1016/S1364-0321(99)00007-6.
[16] A.V. Bridgwater, Review of fast pyrolysis of biomass and product upgrading, Biomass Bioenergy 38 (2012) 68–94, https://doi.org/10.1016/j.biombioe.2011.01.048.
[17] Q. Zhang, J. Chang, T. Wang, Y. Xu, Review of biomass pyrolysis oil properties and upgrading research, Energy Convers. Manage. 48 (1) (2007) 87–92, https://doi.org/10.1016/j.enconman.2006.05.010.
[18] B.V. Babu, Biomass pyrolysis: a state-of-the-art review, Biofuels, Bioprod. Biorefin. 2 (5) (2008) 393–414, https://doi.org/10.1002/bbb.92.
[19] H.B. Goyal, D. Seal, R.C. Saxena, Bio-fuels from thermochemical conversion of renewable resources: a review, Renew. Sustain. Energy Rev. 12 (2) (2008) 504–517, https://doi.org/10.1016/j.rser.2006.07.014.
[20] D.U. Jun, L.I.U. Ping, Z.H. Liu, D.G. Sun, C.Y. Tao, Fast pyrolysis of biomass for bio-oil with ionic liquid and microwave irradiation, J. Fuel Chem. Technol. 38 (5) (2010) 554–559, https://doi.org/10.1016/S1872-5813(10)60044-8.
[21] A.A. Boateng, D.E. Daugaard, N.M. Goldberg, K.B. Hicks, Bench-scale fluidized-bed pyrolysis of switchgrass for bio-oil production, Ind. Eng. Chem. Res. 46 (7) (2007) 1891–1897, https://doi.org/10.1021/ie0614529.
[22] N.J. Parziale, Thermo-chemical biomass conversion by piston compression of surrounding gas, in: Proceedings of the 247th American Chemical Society National Meeting, ACS-ENFL-69, Dallas, Texas, 2014.
[23] N.J. Parziale, Calculation of Input Sensitivities for a Reciprocating Biomass Conversion Reactor (RBCR), in: Proceedings of the 3rd International Energy and Sustainability Conference, IEEE, Farmingdale, New York, 2014.
[24] R. van Basshuysen, F. Schäfer, Internal Combustion Engine Handbook – Basics, Components, Systems, and Perspectives, Society of Automotive Engineers Inc, 2004.
[25] Q. Xue, T.J. Heindel, R.O. Fox, A CFD model for biomass fast pyrolysis in fluidized-bed reactors, Chem. Eng. Sci. 66 (11) (2011) 2440–2452, https://doi.org/10.1016/j.ces.2011.03.010.
[26] M.J. Antal Jr., G. Várhegyi, Cellulose pyrolysis kinetics: the current state of knowledge, Ind. Eng. Chem. Res. 34 (3) (1995) 703–717, https://doi.org/10.1021/ie00042a001.

Please cite this article as: N. J. Parziale and R. Adhikari, Model and sensitivity analysis of the reciprocating biomass conversion reactor (RBCR), International Journal of Heat and Mass Transfer, https://doi.org/10.1016/j.ijheatmasstransfer.2019.118988

[27] G. Várhegyi, M.J. Antal Jr., E. Jakab, P. Szabó, Kinetic modeling of biomass pyrolysis, J. Anal. Appl. Pyrol. 42 (1) (1997) 73–87, https://doi.org/10.1016/S0165-2370(96)00971-0.
[28] C. Di Blasi, Modeling chemical and physical processes of wood and biomass pyrolysis, Prog. Energy Combust. Sci. 34 (1) (2008) 47–90, https://doi.org/10.1016/j.pecs.2006.12.001.
[29] R.S. Miller, J. Bellan, A generalized biomass pyrolysis model based on superimposed cellulose, hemicellulose and liqnin kinetics, Combust. Sci. Technol. 126 (1–6) (1997) 97–137, https://doi.org/10.1080/00102209708935670.
[30] A.G.W. Bradbury, Y. Sakai, F. Shafizadeh, A kinetic model for pyrolysis of cellulose, J. Appl. Polym. Sci. 23 (11) (1979) 3271–3280, https://doi.org/10.1002/app.1979.070231112.
[31] F. Shafizadeh, A.G.W. Bradbury, Thermal degradation of cellulose in air and nitrogen at low temperatures, J. Appl. Polym. Sci. 23 (5) (1979) 1431–1442, https://doi.org/10.1002/app.1979.070230513.
[32] F. Shafizadeh, Introduction to pyrolysis of biomass, J. Anal. Appl. Pyrol. 3 (4) (1982) 283–305, https://doi.org/10.1016/0165-2370(82)80017-X.
[33] S.M. Ward, J. Braslaw, Experimental weight loss kinetics of wood pyrolysis under vacuum, Combust. Flame 61 (3) (1985) 261–269, https://doi.org/10.1016/0010-2180(85)90107-5.
[34] A.G. Liden, F. Berruti, D.S. Scott, A kinetic model for the production of liquids from the flash pyrolysis of biomass, Chem. Eng. Commun. 65 (1) (1988) 207–221, https://doi.org/10.1080/00986448808940254.
[35] L.J. Curtis, D.J. Miller, Transport model with radiative heat transfer for rapid cellulose pyrolysis, Ind. Eng. Chem. Res. 27 (10) (1988) 1775–1783, https://doi.org/10.1021/ie00082a007.
[36] C.A. Koufopanos, A. Lucchesi, G. Maschio, Kinetic modelling of the pyrolysis of biomass and biomass components, Can. J. Chem. Eng. 67 (1) (1989) 75–84, https://doi.org/10.1002/cjce.5450670111.
[37] C.A. Koufopanos, N. Papayannakos, G. Maschio, A. Lucchesi, Modelling of the pyrolysis of biomass particles. Studies on kinetics, thermal and heat transfer effects, Can. J. Chem. Eng. 69 (4) (1991) 907–915, https://doi.org/10.1002/cjce.5450690413.
[38] C. Di Blasi, Numerical simulation of cellulose pyrolysis, Biomass Bioenergy 7 (1–6) (1994) 87–98, https://doi.org/10.1016/0961-9534(94)00040-Z.
[39] I. Milosavljevic, E.M. Suuberg, Cellulose thermal decomposition kinetics: global mass loss kinetics, Ind. Eng. Chem. Res. 34 (4) (1995) 1081–1091, https://doi.org/10.1021/ie00043a009.
[40] Q. Xue, D. Dalluge, T.J. Heindel, R.O. Fox, R.C. Brown, Experimental validation and CFD modeling study of biomass fast pyrolysis in fluidized-bed reactors, Fuel 97 (2012) 757–769, https://doi.org/10.1016/j.fuel.2012.02.065.
[41] F.P. Incropera, D.P. DeWitt, T.L. Bergman, A.S. Lavine, Fundamentals of Heat and Mass Transfer, sixth ed., John Wiley & Sons Incorporated, 2007.
[42] J. Patterson, J. Imberger, Unsteady natural convection in a rectangular cavity, J. Fluid Mech. 100 (1) (1980) 65–86, https://doi.org/10.1017/S0022112080001012.
[43] D.R. Dudek, T.H. Fletcher, J.P. Longwell, A.F. Sarofim, Natural convection induced drag forces on spheres at low grashof numbers: comparison of theory with experiment, Int. J. Heat Mass Transf. 31 (4) (1988) 863–873, https://doi.org/10.1016/0017-9310(88)90143-3.
[44] R.B. Bird, W.E. Stewart, E.N. Lightfoot, Transport Phenomena, first ed., John Wiley & Sons, 1960.
[45] J.H. Lienhard, A Heat Transfer Textbook, fourth ed., Phlogiston Press, 2012.
[46] D.G. Goodwin, An open-source, extensible software suite for CVD process simulation, in: M. Allendorf, F. Maury, F. Teyssandier (Eds.), Proceedings of CVD XVI and EuroCVD Fourteen, 2003, pp. 155–162.
[47] B.J. McBride, M.J. Zehe, S. Gordon, NASA Glenn Coefficients for Calculating Thermodynamic Properties of Individual Species, NASA TP-2002-211556, 2002.
[48] Y.A. Çengel, A.J. Ghajar, Heat and Mass Transfer: Fundamentals & Applications, fourth ed., McGraw-Hill, 2011.
[49] C.C. Sun, True density of microcrystalline cellulose, J. Pharm. Sci. 94 (10) (2005) 2132–2134, https://doi.org/10.1002/jps.20459.
[50] A.V. Blokhin, O.V. Voitkevich, G.J. Kabo, Y.U. Paulechka, M.V. Shishonok, A.G. Kabo, V.V. Simirsky, Thermodynamic properties of plant biomass components. heat capacity, combustion energy, and gasification equilibria of cellulose, J. Chem. Eng. Data 56 (9) (2011) 3523–3531, https://doi.org/10.1021/je200270t.
[51] L.F. Shampine, M.W. Reichelt, The Matlab ODE Suite, SIAM J. Sci. Comput. 18 (1) (1997) 1–22, https://doi.org/10.1137/S1064827594276424.
[52] C.A. Mullen, A.A. Boateng, N.M. Goldberg, I.M. Lima, D.A. Laird, K.B. Hicks, Bio-oil and bio-char production from corn cobs and stover by fast pyrolysis, Biomass Bioenergy 34 (1) (2010) 67–74, https://doi.org/10.1016/j.biombioe.2009.09.012.
[53] S. Mani, L.G. Tabil, S. Sokhansanj, Grinding performance and physical properties of wheat and barley straws, corn stover and switchgrass, Biomass Bioenergy 27 (4) (2004) 339–352, https://doi.org/10.1016/j.biombioe.2004.03.007.
[54] R.H. Perry, C.H. Chilton, Chemical Engineers' Handbook, fifth ed., McGraw Hill Book Company, 1973.
[55] S. Papari, K. Hawboldt, A review on condensing system for biomass pyrolysis process, Fuel Process. Technol. 180 (2018) 1–13, https://doi.org/10.1016/j.fuproc.2018.08.001.

Please cite this article as: N. J. Parziale and R. Adhikari, Model and sensitivity analysis of the reciprocating biomass conversion reactor (RBCR), International Journal of Heat and Mass Transfer, https://doi.org/10.1016/j.ijheatmasstransfer.2019.118988